Comparative study of a nano-bacterial rat kidney stone model and the traditional ethylene glycol rat kidney stone model

Biao Qian (qb2003_2000@163.com)
Jingshen wang
shihezi university
Zhiqiang Hao
Shihezi University School of Medicine
Yuan Wang
Shihezi University School of Medicine
Heng Yang
Shihezi University School of Medicine
Yongle Li
Shihezi University School of Medicine
Minghui Tan
Shihezi University School of Medicine
Guoxi Zhang
First Affiliated Hospital Of Gannan Medical College
Xiaofeng Zou
First Affiliated Hospital Of Gannan Medical College

Research

Keywords: Kidney stones, Nanobacteria, Ethylene glycol, Rat model

Posted Date: March 11th, 2020

DOI: https://doi.org/10.21203/rs.3.rs-16816/v1

Abstract

Objective To Compare a nanobacterial (NB) rat kidney stone model and the traditional ethylene glycol (EG) rat kidney stone model to assess its significance.

Methods Ninety Wistar male rats were randomly divided into three groups. After the first week of modeling, three rats of every groups were randomly selected to measure the biochemical blood and urine markers. After the sacrifice, the renal tissues were observed to assess the pathological changes. The expression levels of CaSR and Claudin-14 protein were detected by kinds of technology.

Results The biochemical metabolic indices of rats in NB group began to increase at the third week and decreased to normal at the 9th week. In the EG group they began to increase at the second week and did not return to normal later. At the 7th week, the creatinine levels of rats in the EG group were higher than in the NB group, and the difference was statistically significant. The formation rates of kidney stones in the NB group and EG group were 52.4 and 66.7%, respectively, but the difference of the two rates was not statistically significant. The protein expression CaSR and Claudin-14 in the EG group began to strengthen at 3rd week, and at 4th week in the NB group. CaSR was continuously expressed in the NC group, but Claudin-14 was not expressed.

Conclusion The formation of stones in the NB group began slightly later. CaSR and Claudin-14 proteins play a role in the formation of kidney stones.

Background

Kidney stones are a common urological disease. However, their etiology is complicated and not yet fully understood. The establishment of a successful and suitable kidney stone animal model is the basis for studying its formation mechanism[1]. The EG rat kidney stone model is a traditional approach that has been used as one of the classic research models [2]. After entering the body, EG is converted into oxalic acid through various pathways, and oxalic acid combines with calcium in urine to form calcium oxalate crystals [3]. Ammonium chloride enters the body to acidify the urine [4], which causes the function of the renal tubular cells to be impaired, which is conducive to the formation of kidney stone crystals.

In recent years, studies have found that nanobacteria are associated with a variety of calcification-related diseases, and have become a candidate for a cause of the formation of kidney stones. The nanobacteria were discovered by the team of the Finnish scientist Kajander[5]. Their diameter is between 80 and 500 μm, which makes them the smallest presently known living organisms, inspiring the name nanobacteria (NB). Shiekh et al.[6] confirmed in animal experiments that nanobacteria are involved in the pathogenesis of renal tubular calcification. Our group[7] collected nanobacteria from the urine of patients with upper urinary tract stones in the early stage, and injected them into the tail vein of rats to establish a rat kidney stone model.

In recent years, studies have found that the CaSR-Claudin-14 pathway is closely related to renal calcium reabsorption and kidney stone formation[8]. CaSR is a G-protein coupled receptor that is significantly associated with urinary calcium excretion, where it plays a role by inhibiting renal tubular reabsorption of calcium by upregulating the expression of Claudin-14 in thick ascending limbs (TAL)[9]. In order to further study the etiology of kidney stones, a nano-bacterial kidney stone model was established in this study. At the same time, an ethylene glycol-induced rat kidney stone was established by using ethylene glycol in conjunction with ammonium chloride a stimulating agent. We observed the formation of kidney stones in the two models and assessed biochemical markers in the blood and urine, as well as ultrastructural changes related to kidney damage to explore the differences between the behavior of the two proteins in the two modeling methods.

1 Materials And Methods

1.1 Experimental animals

A total of 90 specific-pathogen-free (SPF) male Wistar rats of 6 weeks old and weighing (200 ± 20) g, were obtained from Xinjiang Medical University Experimental Animal Center, Xinjiang, China (certificate number SCXK (new) 2013-0001; new medical verb SYXK (new) 2010-0003, welfare ethics review certificate number: [2016] Court trial (001) (NO) A2016-001).

2 Experimental Methods

2.1 Establishment of rat kidney stone models

2.1.1 Experimental grouping and processing

The rats were randomly divided into 3 groups: control group (NC group: tail vein injection saline 1.2 mL + saline 2mL gavage); ethylene glycol group (EG group: tail vein injection saline + 1% ethylene glycol drinking water and 2% ammonium chloride AC 2mL gavage); NB group (NB group: tail vein injection NB1.2mL + saline 2mL gavage). The drug was injected once a day for seven consecutive days.

2.1.2 Collection of experimental animal specimens

Three rats were randomly selected from each group every week from the first week to the end of the tenth week after the injection of nanobacteria or ethylene glycol treatment. The urine was collected for 24 hours in each group using a metabolic cage. 10% pentobarbital was injected intraperitoneally at 30 mg / kg. Open the abdominal cavity aseptically, remove 4 mL of inferior vena cava blood, and then kill the rat. After the rat heart stopped beating, bilateral kidneys were removed. Frozen one side of the kidney and the other side fixed with a neutral formaldehyde solution.

2.2 Kidney stone formation

The whole kidney was observed with the naked eye, and the size, color, and shape, as well as the presence or absence of stones were assessed. Then, the shape of the kidney and the formation of kidney

stone crystals were observed using a dissecting microscope.

2.3 Analysis of biochemical markers from the blood and urine

The collected blood and urine specimens were examined for biochemical indices including, Serum creatinine, uric acid, urea, blood calcium, blood phosphorus, blood magnesium, urine Ph, urinary calcium, urine specific gravity and 24-hour urine output, using a automatic biochemical analyzer.

2.4 Observation of renal pathological changes

Kidney specimens were fixed, cut into 4 μm sections using cryomicrotome, and stained with HE. The distribution and number of crystals in the kidney and the changes of renal tubules and surrounding tissues were observed under an optical microscope.

2.5 Measurement of CaSR and Claudin-14 mRNA expression by qRT-PCR

Samples comprising approximately 100 mg of kidney tissue were cut and placed it into RNase-free 1.5 ml Eppendorf tubes. After lysis with Trizol reagent and three high-speed centrifugation steps at 4°C, the pellet was dried on ice and resuspended in 20 μL DEPC water. The RNA concentration was measured using a nucleic acid and protein detector, reverse-transcribed into cDNA using a commercial kit, and stored in a refrigerator at -20 °C until use. The PCR reaction was carried out in a 20 μL system, and the temperature program encompassed pre-denaturation at 95°C for 1 min, followed by 40 cycles of 95°C for 15 s, 60°C for 30 s and 72°C for 30 s. The results were expressed by measuring the average Ct value three times for each sample. The primers were designed using Primer Premier 5.0 software, and the sequences are shown in Table 1.

2.6 Immunohistochemical staining for CaSR and Claudin-14 protein expression

The kidneys with clear pathological hallmarks of successful model induction were used for immunohistochemistry, which was performed using the SP method. The samples were embedded in paraffin and sliced into 4-μm sections, followed by routine de-waxing, H_2O_2 treatment to deactivate endogenous peroxidases, incubation in Tannic acid buffer to regenerate the antigens, and blocking with serum. The anti-CaSR antibody (1:150) or the anti-Claudin-14 antibody (1:150) was added drop-wise, and incubated overnight at 4 °C. The goat anti-mouse and rabbit anti-goat secondary antibody was added drop-wise, and color development was controlled under a DAB microscope. The samples were counterstained with hematoxylin, dehydrated with different concentrations of ethanol and xylene, sealed with gum, and observed under a microscope within 1 to 10 weeks.

2.7 Western blot analysis of CaSR and Claudin-14 expression

Each sample comprising about 200 mg of kidney tissue was placed in an EP tube and finely ground on ice. After centrifugation at 4°C for 3 times, the supernatant was recovered as the total protein extract of the tissue, and placed in a -80°C refrigerator. The total cytoplasmic protein concentration of the kidney

tissue was measured using a BCA kit, followed by loading of an appropriate amount, electrophoresis (collecting gel 20 mA, separation gel 35 mA), and electrotransfer to a membrane (100 mA, 40 min). The membrane was stained with Ponceau, and the gel was stained with Coomassie brilliant blue. Color development was performed using a western blot kit.

3 Statistical Analysis

SPSS 22.0 (IBN Corp., USA) was used for statistical analysis. The data were expressed as $\bar{x} \pm s$. The measurement data of rats in each group were analyzed by analysis of variance. The data of two groups were compared using the χ^2 test. The rate of crystal formation in each group was compared using the rank sum test. The Kruskal Wallis test was used with a standard of $\alpha = 0.05$.

4 Results

4.1 Formation of kidney stones in each group

No kidney stones were found in either of the groups 2 weeks before model establishment. At the beginning of the third week, transparent crystals were formed in the EG group. They were mainly distributed in the distal and proximal convoluted tubules. The crystals were irregularly shaped or agglomerated. At the beginning of the fourth week, the NB group showed the same appearance of crystals in the distal and proximal convoluted tubules as the EG group, but their number was smaller than. There was no significant difference in the stone formation rate between the two groups (P>0.05). During the entire duration of the modeling process, no stones were observed in the NC group (Table 2).

Tips：Because this was a dynamic study, a group of rats had to be sacrificed every week, and the formation of kidney stones requires a certain time. Kidney stones appeared in the 4th week in the NB group, and in the 3rd week of the EG group. There is the possibility of forming stones in that rats have been killed in the first few weeks. Therefore, we excluded the rats that were killed in the previous weeks.

4.2 Comparison of biochemical indicators in blood and urine samples from each group

4.2.1 Comparison of blood biochemical indicators in each group of rats

At 3-8 weeks, creatinine, uric acid and urea in the NB group increased to different degrees, becoming significantly higher than in the NC group (P<0.05), but decreased slightly in the 9th-10th week. There was no significant difference compared to the NC group. In the EG group, creatinine, uric acid and urea increased in the second week, was and the difference from the NC group was statistically significant (P<0.05). At 7-10 weeks, there was a difference in creatinine between the EG group and NB group. The levels of calcium, phosphorus, and magnesium in the blood, as well as the urine pH were higher in the EG group and NB group than in the NC group at some time points (P<0.05; figure 1).

4.2.2 Comparison of urine biochemical indicators

Urinary calcium levels gradually increased in the NB group from week 1 to week 8, and subsequently decreased slightly in the 9th and10th week. Statistical comparisons between the two groups showed that there was a statistically significant difference in urinary calcium between the 3rd and the 9th week ($P<0.05$), but there were no significant differences in the other weeks. There was no significant difference in the 24h urine volume and urine specific gravity ($P>0.05$). Urinary calcium levels in the EG group increased significantly from the 2nd week to the 7th week. Compared with the NC group, the difference was statistically significant ($P<0.05$). However, there was no significant change in the other weeks. The 24h urine volume and urine specific gravity of the NB group and EG group were not significantly different from those of the NC group ($P>0.05$; Figure 2).

4.3 Comparison of renal pathological changes in each group of rats

Two weeks before modeling, there were no obvious changes in the pathological examination of frozen sections of each group, and there was no crystal formation. In the third week, mild expansion of renal tubular epithelium was observed in the EG and NB groups, and epithelial cells showed granular degeneration. The change in the EG group was more severe than in the NB group, and a small amount of transparent crystals appeared, located in the collecting tubes. As expected, there were no pathological changes or crystal formation in the control group. At the 4th week, small amounts of transparent crystals appeared in the NB group. The interstitium and the renal tubules of the EG and NB groups expanded significantly. There was obvious vacuolar degeneration of cells, swelling of the epithelial cells, and transparent crystals in the renal tubules, collecting ducts and among the renal interstitial cells. In some areas, there were clumps, pieces, or irregular fragments. At the same time, renal tubular epithelial detachment occurred, and lymphocytes infiltration in the renal interstitium and the renal capsule was observed sporadically. Furthermore, with the prolongation of modeling time, the kidney damage was further aggravated, and the number of formed crystals further increased. The degree of damage in the NB group was lower than in the EG group, and fewer crystals were formed. During the whole modeling period, no obvious pathological changes were observed in the kidneys of the blank control group, and no formation of kidney stone crystals was observed (Figure 3).

4.4 Measurement of CaSR and Claudin-14 mRNA expression in renal tissues of each group by qRT-PCR

As shown in Figure 2, the expression of CaSR mRNA in renal tissues of the EG and NB groups increased significantly, and the expression of CaSR mRNA in the EG group was higher than that in the NB group. CaSR mRNA was significantly expressed in the kidney tissue of the NC group. The expression of Claudin-14 mRNA in the kidney tissues of EG group and NB group was significantly higher than in the NC group. The expression of Claudin-14 mRNA in the EG group was higher than in the NB group (figure 4).

4.5 Immunohistochemical detection of CaSR and Claudin-14 protein expression

4.5.1 Immunohistochemical detection of CaSR expression

Observation of immunohistochemically stained sections under the light microscope showed that CaSR was continuously expressed in the kidney tissues of the three groups of rats. From the third week, the expression of CaSR protein in the kidney tissue of the EG group was significantly enhanced. From the 4th week, expression was observed in the kidney tissue of the NB group. The expression of CaSR protein began to increase, and it was diffusely distributed on the cell membrane of renal tubular epithelial cells, which was brown. The expression of CaSR in kidney tissue of the EG group was obviously stronger than in the NB group. During the 10 weeks, CaSR was continuously expressed in the NC group, but the intensity did not change significantly (Figure 5).

4.5.2 Immunohistochemical detection of Claudin-14 expression

Claudin-14 was continuously expressed in the kidney tissues of the EG and NB groups, but not in the samples of the NC group. The expression of Claudin-14 protein in renal tissue of the EG group significantly increased from the 3rd week. From the 4th week, the expression of Claudin-14 protein in the kidney tissue of the NB group also began to increase, and immunoreactivity was diffusely distributed on the cell membrane of renal tubular epithelial cells, showing a brown color. The expression of Claudin-14 protein in the EG group in each week was significantly stronger than in the NB at all time points (Figure 6).

4.6 Western blot analysis of CaSR and Claudin-14 protein expression in kidney tissues of each group

Densitometric analysis of the immunoblots in Quantity One software revealed that CaSR was expressed in the kidney tissues of the three groups of rats, but the was significantly higher in the EG and NB groups than in the NC group. Moreover, the expression of CaSR was significantly higher in the EG group than in the NB group. The expression of Claudin-14 in the kidney tissues of the EG and NB groups was significantly higher than in the NC group. Similar to CaSR, the expression of Claudin-14 was higher in the EG group than in the NB group (Figure 6).

5 Discussion

Kidney stones are mostly composed calcium oxalate[10]., and many factors can lead to their formation [11]. In order to study the mechanism of the pathogenesis of kidney stones, it is necessary to establish animal models. At present, models of kidney stones in rats are mainly established by means of drugs[12]. The most common method uses the intragastric administration of ethylene glycol and ammonium chloride. With the increase of research on nanobacteria (NB), it was discovered that they are the only known organisms that can produce hydroxyapatite in human body[13]. In order to study the role of nanobacteria in the formation of kidney stones, an animal model was successfully constructed using NB cultured from the urine of patients with kidney stones[14]. In order to further study the value and significance of the establishment of animal models based on nanobacteria for the etiology of kidney

stones, this study used two methods to construct kidney stone models in male Wistar rats and compare the differences between the two modeling methods.

There were 2 deaths in the EG group, probably because ethylene glycol compounded the toxic effects of ammonium chloride [4]. The formation of stones in the EG group was earlier than in the NB group, but there was no significant difference in the rate of stone formation between the two groups. Analysis of biochemical markers in the blood and urine showed that serum creatinine, serum uric acid, urea nitrogen and urinary calcium levels were higher in the EG and NB groups than in the NC group, and these indicators changed significantly earlier in the EG group than in the NB group. No recovery was seen, and the indicators fell to normal levels in the NB group during the later experimental period. In the early stage of modeling, the biochemical results of the NB group did not indicate damage to the renal function or only low-level damage. It can be seen that the damage to the kidneys induced by NB was obviously lighter than in the EG group, and it could be recovered in the later stage of modeling, whereby the morphology of the kidney was changed. This phenomenon is consistent with an earlier report[15], indicating that modelling using ethylene glycol in conjunction with ammonium chloride produces more serious kidney damage[16], and has a greater impact on renal function. By contrast in the nanobacteria-induced model, the renal damage may be caused by secondary damage to renal tubular epithelial cells after the formation of kidney stones, and the process of kidney stone formation induced by NB, which is a long-term slow process, is less hash than the formation of stones due to ethylene glycol and ammonium chloride.

Two weeks before model establishment, no significant changes were observed in the pathological examination of each group, and no crystal formation was observed. At the third week, pathological changes were observed in the EG and NB groups, whereby the symptoms of the EG group were more severe than those of the NB group. Small amounts of transparent crystals were located in the collecting tubes, and the control group had no pathological changes or crystal formation. At the 4th week, crystals appeared in the nano-bacteria group. The kidney damage in the EG and NB groups was further aggravated, and the number of formed crystals further increased. The degree of damage in the NB group was lower than in the EG group, and the amount of formed crystals was smaller. During the whole modeling period, the kidneys of the blank control group showed no obvious pathological changes, and no formation of the kidney-stone crystals was observed. This result was consistent with the pathological changes of traditional glycol modeling[17] as well as the pathological changes of nanobacterial modeling.

In this study, the mRNA and protein expression levels of CaSR and Claudin-14 in renal tissues of the EG and NB groups were significantly higher than in the NC group, and the results of qRT-PCR, immunohistochemistry and western blot analysis were all in agreement. The expression of CaSR and Claudin-14 was significantly higher in the EG group than in the NB group, which may be due to damage to the renal tubular epithelium caused by ethylene glycol and ammonium chloride in the early stage of modeling[18]. By contrast, in the NB group, which uses nanobacteria under physiological conditions, the crystal shell of hydroxyapatite can be formed. After formation of this mineralized shell, the nanobacteria

enter a dormant state. After resuscitation, the bacteria can invade or infect tubular cells through a similar receptor-mediated pinocytosis process[19], and this process causes less damage to renal tubular epithelial cells compared with ethylene glycol and ammonium chloride. This indicated that NB may cause the change of CaSR-Claudin-14 channel in a similar manner to ethylene glycol with ammonium chloride. The CaSR-Claudin-14 regulatory pathway may play a role in the formation of kidney stones in both models.

At present, the key basis of various animal models of kidney stones is tubular cell damage[20], which is one of the main theories of the pathogenesis of kidney stones [21]. Vervaet et al. found that renal tubular epithelial cell damage can be observed in the early stage of kidney stone formation[22, 23]. Due to cell damage, crystals are more likely to adhere to cells, thereby forming stones, accompanied by damage to renal tubular epithelial cells. The tight junction of the cells are destroyed, the polarity of the cell membrane is changed, and the cell's secondary protective coating is reduced[24], which further enhances the adhesion of the crystals and kidney stone formation. In addition, after the formation of the kidney stone crystals, the tubular epithelial cells are continuously compressed, resulting in cell damage. Ischemia, hypoxia and mechanical damage increase the risk of tubular epithelial cell damage[25]. Ethylene glycol is a commonly used stone-promoting agent in rat kidney stone models. After entering the body, it is converted into oxalic acid through multiple pathways under the catalysis of various enzymes [3]. Ammonium chloride enters the body and damages the renal tubular epithelial cells, creating conditions for the formation of kidney stone crystals. NB form a hydroxyapatite shell under their own unique physiological influence. At the same time, NB enter a dormant state. When NB enter the body, they induce a series of inflammatory pathological reactions through receptor-mediated pinocytosis, which leads to cell injury[26].

Yu et al. confirmed that NB can cause damage to co-cultured human renal tubular epithelial cells, and found that NB-induced damage to renal tubular epithelial cells is a progressive process[27]. The adhesion of the cells to the crystals is further enhanced, and the necrotic epithelial cell debris further promotes the nucleation of the kidney stone crystal[28, 29]. With prolonged time, the formation of crystals increased, and the structure of renal tubules showed more obvious pathological changes, which was consistent with the experimental observation of renal tubular and peripheral cell injury[30], further demonstrating the damage caused by NB to renal tubular epithelial cells. This in turn enhances the adhesion and deposition of renal tubular epithelial cells. However, whether the nanobacteria first form a calcified lesion and then damages the renal tubular epithelial cells, or first damage the renal tubular epithelial cells which in turn induces the formation of kidney stones requires further study.

The etiology of kidney stones is complex and the animal models are diverse. The discovery of nanobacteria brought a completely new paradigm for the study of kidney stones and needs further research. The results of this study inidicate that the traditional method of modeling kidney stones with ethylene glycol induces serious damage to kidney function and forms more crystals. It is suitable for experiments requiring short-term stone formation and large number of stones but have low requirements in terms of renal function. The process of kidney stone formation induced by nanobacteria is less harsh,

the damage to renal function is lower, the modeling time is long, and the number of formed crystals is lower. Importantly, the nanobacteria had little effect on the experimental animals, and the formation process of the kidney stones is more in line with the natural process of the disease. This potentially makes the NB model more conducive to the study of the etiology of kidney stones, and therefore certainly merits further research.

Conclusion

NB can lead to the formation of kidney stones, which is not significantly different from the ethylene glycol modeling method. The CaSR and Claudin-14 proteins in the NB group and the EG group increased to varying degrees during the formation of stones, which may indicate that the two proteins are risk factors for the formation of kidney stones. The specific mechanism needs further experimental proof.

Declarations

Ethics approval and consent to participate

Medical Ethics Committee of the First Affiliated Hospital of Shihezi University Medical College(A-2019-037-01)

Consent for publication

All authors are informed and agree to publish

Availability of data and materials

The datasets used or analysed during the current study are available from the corresponding author on reasonable request.

Competing interests

There are no financial or other relations that could lead to a conflict of interest.

Funding

This study was supported in part by a grant from the National Natural Science Foundation of China [NO. 81460140].

Authors' contributions

QIAN B and ZOU X.F. conceived and designed the study. WANG J.S. ,HAO Z.Q. ,WANG Y and YANG H performed the experiments. LI Y.L.and TAN M.H. wrote the paper. QIAN B and ZHANG G.X. reviewed and edited the manuscript. All authors read and approved the manuscript.

Acknowledgements

Acknowledge anyone who contributed towards the article who does not meet the criteria for authorship including anyone who provided professional writing services or materials.

References

1. Wang Ning, Yang Huan, Chen Zhiqiang, et al. Progress in the application of fruit fly model in the study of kidney stones [J]. Chinese Journal of Experimental Surgery, 2016, 37 (5): 398-400.
2. Zeng Chunhui, Li Xianmei, Cai Nina, et al. Study on mouse model of calcium oxalate-type kidney stones[J]. World Journal of Traditional Chinese Medicine, 2016,11(11): 2213-2215.
3. Fassnacht M, Libe R, Kroiss M, et al. Adrenocortical carcinoma: a clinician's update [J]. Nat Rev Endocrinol, 2011, 7.(6):323-325.
4. Huang Youxia, the application of ethylene glycol and ammonium chloride in the establishment of rat kidney calcium oxalate stone model [J]. Strait Pharmaceutical, 2014, 26 (1): 48-49.
5. Kajander E.O. Culture and detection method for sterile filterable autonomously replicating biological particles [J]. U S Patent, 1992, 135:851 .
6. Shiekh F A, Khullar M, Singh S K. Lithogenesis: induction of renal calcifications by nanobacteria. [J]. Urological Research, 2006, 34(1): 53-57.
7. Geng Hao, Wang Qinzhang, Qian Cheng, et al. The application value of Mirco-CT in the study of rat kidney stones[J], Journal of Clinical and Experimental Pathology, 2017, 33(8): 929-931.
8. Sun Wen, Wang Qinzhang, Ding Guofu et al. Expression and significance of calcium sensitive receptor and tight junction protein-14 in renal tissues of calcium oxalate stone[J]. Tianjin Medical Journal, 2014, 42 (7): 657 -660.
9. Dimke H, Desai P, Borovac J, et al. Activation of the Ca2+-sensing receptor increased renal claudin-14 expression and urinary Ca2+ excretion [J]. Am J Physiol Renal Physiol, 2013, 304(6): 761 -769.
10. Deng Yaoliang, Tao Zhiwei, Wang Xiang. Risk factors and individualized prevention and treatment strategies for recurrence of calcium-containing kidney stones [J]. Journal of Clinical Urology, 2018, 02 (33), 85-88.
11. Worcester EM, Coe FL. Clinical practice. Calcium kidney stones [J]. N Engl J Med, 2010, 363(10): 954-963.
12. Taguchi K, Okada A, Yasui T, et al. Pioglitazone, a peroxisome proliferator activated receptor gamma agonist, decreases renal crystal deposition, oxidative stress and inflammation in hyperoxaluric rats [J]. J Urol, 2012, 188(3) :1002-1011.
13. Dong Antao, Gu Jiang, Zhang Yongchun. Analysis of the status quo of urinary calculi induced by nanobacteria[J]. Journal of Clinical Rational Medicine, 2018, 11 (02): 180-181.
14. Geng Hao, Wang Qinzhang, Wu Shuang, et al. Dynamic study of kidney stone formation time in nano-bacterial rat kidney stone model[J].Chinese Journal of General Practice,2017,20(21):2613-

2618.

15. Khan, S.R. Crystal-induced inflammation of the kidneys: results from human studies, animal models, and tissue-culture studies. Clinical and experimental nephrology, 2004. 8(2): p. 75-88.
16. Hao Zhiqiang, Wang Qinzhang, Ni Wei, et al. Dynamic comparison of blood and urine biochemistry in two modeling methods of kidney stones[J]. Chinese Journal of Comparative Medicine, 2018, 28(10): 15-19.
17. Mo L, Huang HY, Zhu XH, et al. Tamm- Horsfall protein is a critical renal defense factor protection against calcium oxalate crystal formation. Kidney Int, 2004, 66(3): 1159-1166.
18. Fassnacht M, Libe R, Kroiss M, et al. Adrenocortical carcinoma: a clinician's update. Nature reviews Endocrinology. 2011 Jun;7(6):323-35. doi: 10.1038/nrendo.2010.235. PubMed PMID: 21386792 ; eng.
19. Kajander EO, Ciftcioglu N, Miller-Hjelle MA, et al. Nanobacteria: controversial pathogens in nephrolithiasis and polycystic kidney disease. Current opinion in nephrology and hypertension. 2001 May;10(3):445-52. PubMed PMID: 11342811; eng
20. TAN Jin, DENG Suiping, OUYANG Jianming. Differences in phagocytosis of calcium oxalate crystals before and after HKC cell injury[J]. Journal of Inorganic Chemistry, 2010, 26(12): 2131-2137.
21. Stefano GB, Challenger S, Kream RM. Hyperglycemia-associated alterations in cellular signaling and dysregulated mitochondrial bioenergetics in human metabolic disorders [J]. Eur J Nutr, 2016, 2(2): 1-7.
22. Vervaet B A, Verhulst A, Broe M E D, et al. The tubular epithelium in the initiation and course of intratubular nephrocalcinosis [J]. Urological Research, 2010, 38(4): 249-256.
23. Vervaet BA, D'Haese PB M. Crystalluric and tubular epithelial parameters during the onset of intratubular nephrocalcinosis: illustration of the 'fixed particle' theory in vivo. [J]. Nephrology Dialysis Transplantation, 2009,24(24): 3659-3668.
24. Xin Wenhu, star. Research progress in the formation of renal tubular epithelial cell damage and calcium oxalate kidney stones [J]. International Journal of Urology, 2013, 33(4).539-542.
25. Rule AD, Bergstralh EJ, 3rd MLJ, Li X, Weaver AL, Lieske JC. Kidney stones and the risk for chronic kidney disease [J]. Clin J Am Soc Nephrol. 2009,4(4): 804-11 .
26. Zheng Yongbo, Wu Chengtang, Huang Xiangcheng. Research progress of nanobacteria[J]. Chinese Journal of Microbiology and Immunology, 2003, 23(11): 914-915.
27. Cheng-Fan YU, Huang XB, Chen L, et al. Effect of nanobacteria on cell damage and crystal retention in renal tubular epithelial cells [J]. Journal of Peking University, 2010, 42(4): 436-442 .
28. Adam P, Hahner S, Hartmann M, et al. Epidermal growth factor receptor in adrenocortical tumors: analysis of gene sequence, protein expression and correlation with clinical outcome. [J]. Modern Pathology An Official Journal of the United States & Canadian Academy of Pathology Inc, 2010, 23(12): 1596-1604.

29. Xu YZ, Zhu Y, Shen ZJ, et al. Significance of heparanase-1 and vascular endothelial growth factor in adrenocortical carcinoma angiogenesis: potential for therapy. [J]. Endocrine, 2011, 40(3): 445-451 .
30. Wang Yihe, Wang Qinzhang, Wu Shuang, et al. The role of nanobacteria in the damage of renal tubular epithelial cells in the formation of kidney stones [J]. Chinese General Practice, 2018, 21 (35): 4364-4370.

Tables

Table 1 Primers used for qRT-PCR of the β-actin, CaSR and Claudin-14 genes.

Gene	Primer sequence
β-actin	Forward CAACCTTCTTGCAGCTCCTC
	Reverse CGGTGTCCCTTCTGAGTGTT
CaSR	Forward CTTTGTGCTGGGTGTCTTCA
	Reverse AACAAGGAGCTGGAGAAGCA
Claudin-14	Forward CTCTGCATGGTGGCTGTCT
	Reverse GGAGATGAAGCCGAGGTACA

Table 2 Assessment of the presence or absence of stones in the kidney tissue samples from each group

Group	n	Positive	Negative	Kidney stone formation rate
EG	24	8	16	66.7
NB	21	10	11	52.4
NC	30	30	0	0

Figures

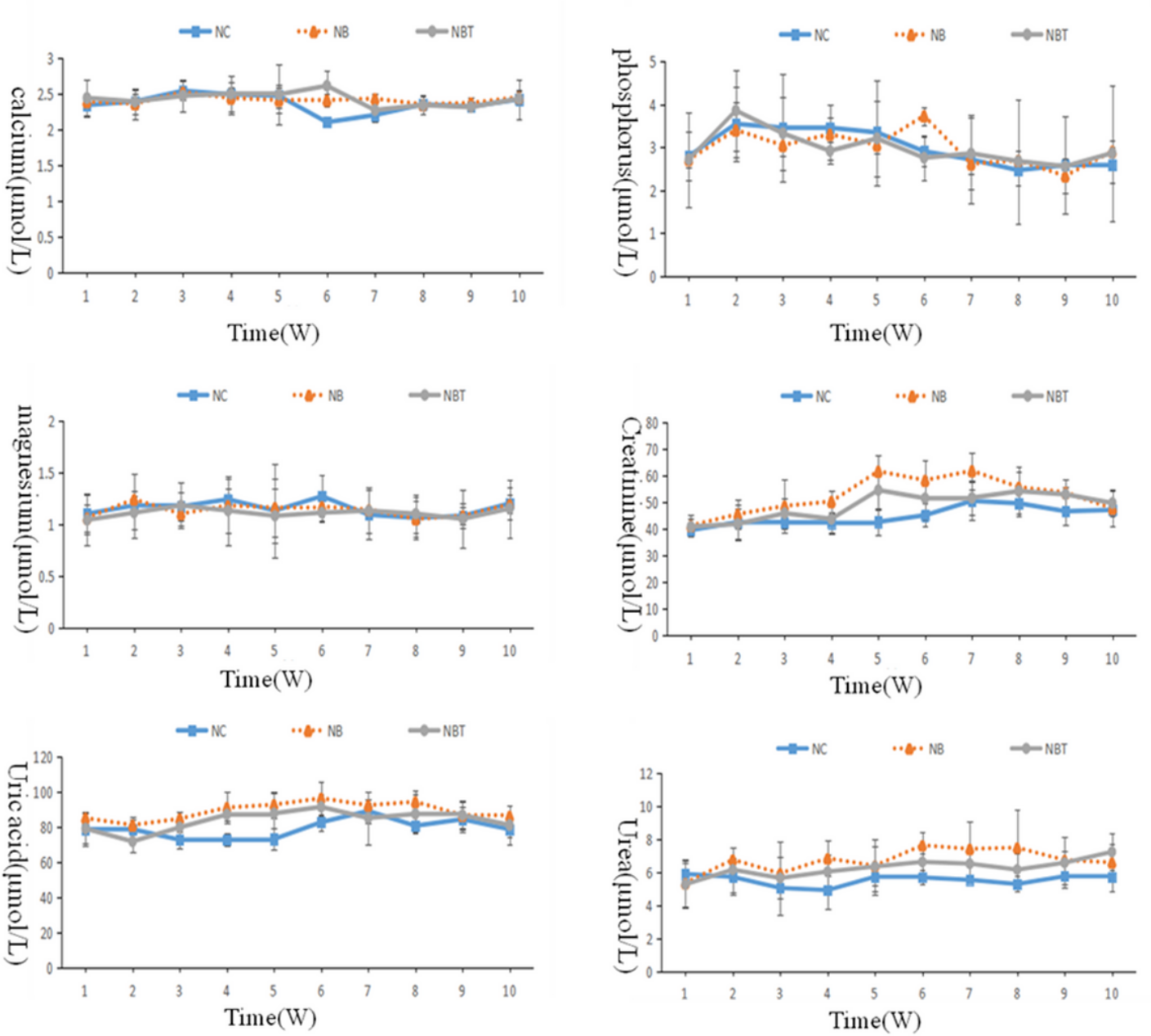

Figure 1

Comparison of biochemical blood markers in the NB, EG and NC groups

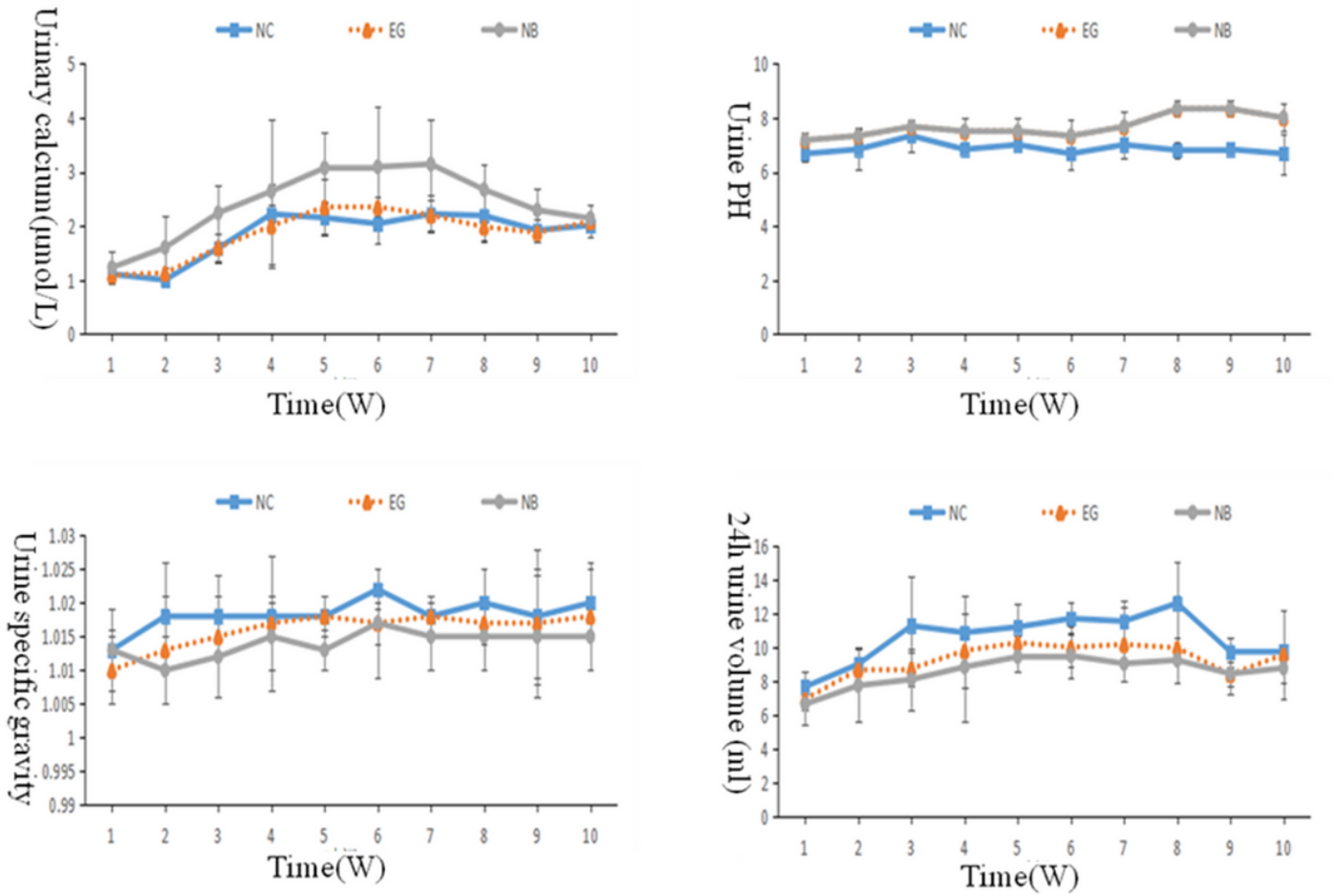

Figure 2

Comparison of biochemical urine markers between the NB, EG and NC groups

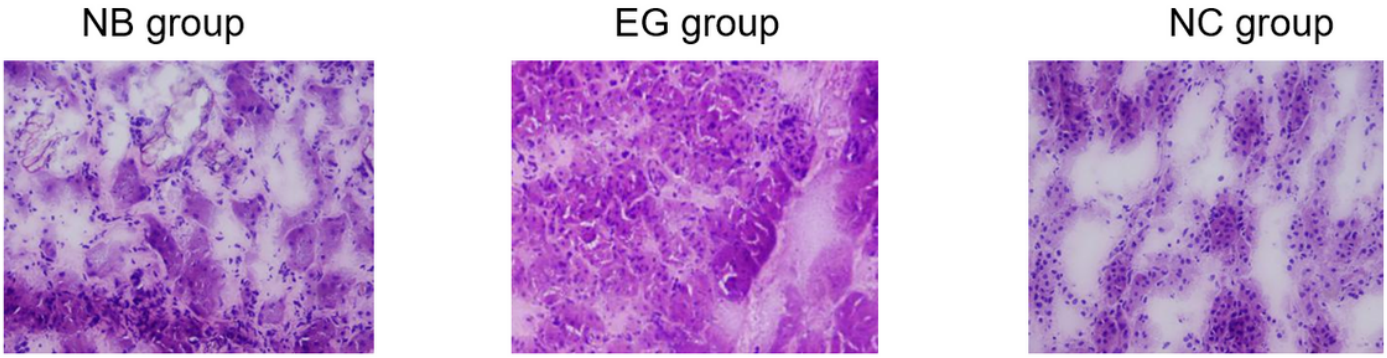

Figure 3

Frozen sections of kidneys in each group (HE × 200)

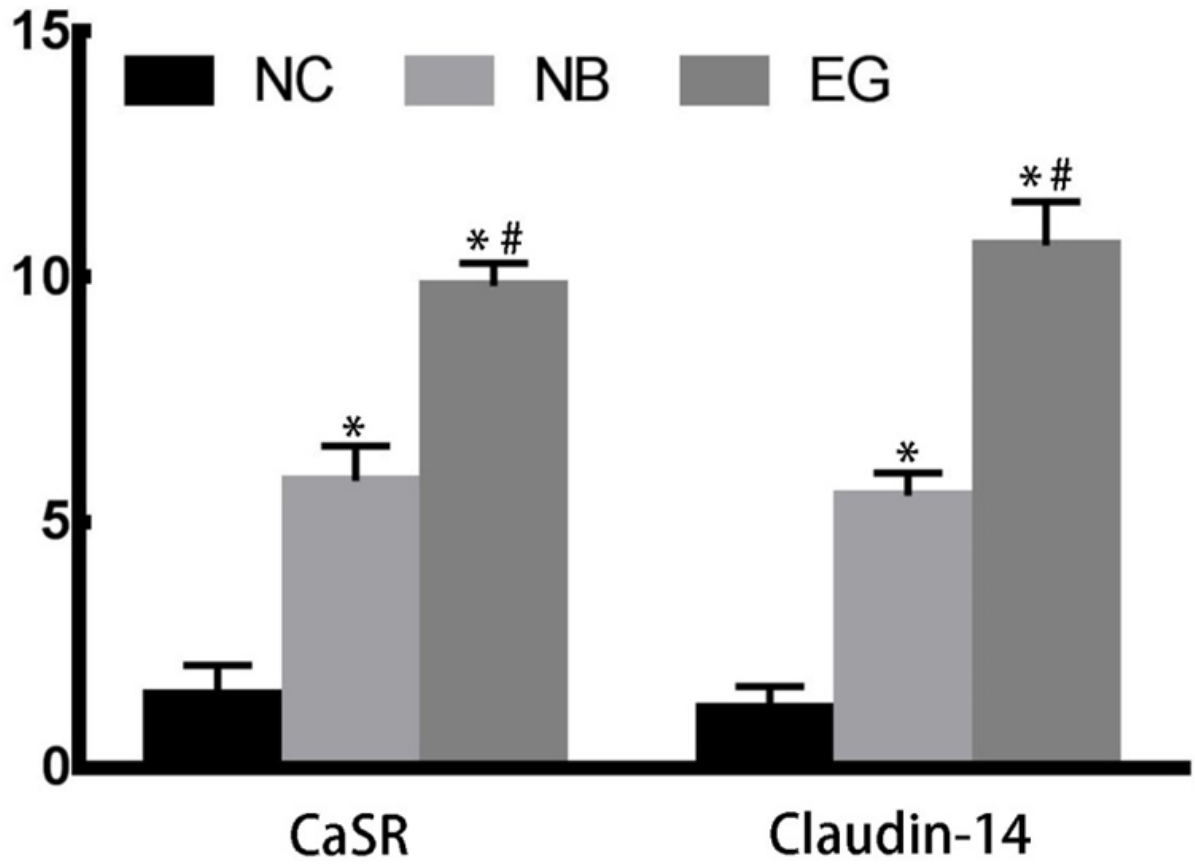

Figure 4

Expression of CaSR and Claudin-14 mRNA in kidney tissues in the three groups of rats on the eighth week. *P<0.05 compared with the NC group, # P<0.05 compared with the NB group.

Figure 5

Positive expression of CaSR and Claudin-14 in the kidney tissues of all three groups of rats at the 8th week (immunohistochemistry; magnification ×200).

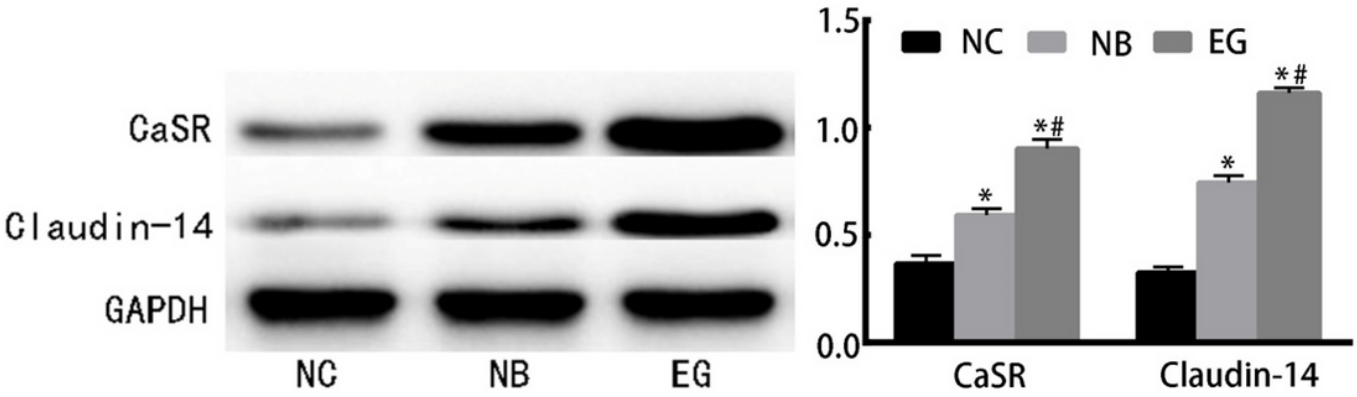

Figure 6

Western blot analysis of CaSR and Claudin-14 protein expression in kidney tissues of the three groups of rats on the eighth week. *P<0.05 compared with the NC group, # P<0.05 compared with the NB group.